Available online at www.sciencedirect.com
ScienceDirect
Polymer 48 (2007) 5889–5895
polymer
www.elsevier.com/locate/polymer

Blue light-emitting diodes from mesogen-jacketed polymers containing oxadiazole units

Ping Wang, Chunpeng Chai, Yutao Chuai, Fuzhi Wang, Xiaofang Chen, Xinghe Fan*, Yiding Xu, Dechun Zou*, Qifeng Zhou*

Beijing National Laboratory for Molecular Sciences, Key Laboratory of Polymer Chemistry and Physics of Ministry of Education, College of Chemistry and Molecular Engineering, Peking University, Beijing 100871, China

Received 12 May 2007; received in revised form 28 July 2007; accepted 30 July 2007
Available online 6 August 2007

Abstract

A series of novel mesogen-jacketed polymers, poly{2,5-bis[(5-*tert*-butylphenyl)-1,3,4-oxadiazole]styrene} (P-Ct) and poly{2,5-bis-[(5-alkoxyl-phenyl)-1,3,4-oxadiazole]styrene} (P-OC*n*, *n* is the number of carbons in the alkoxyl groups, $n = 6$, 8, 10, 12, 14), were incorporated into polymer light-emitting device as the light-emitting layers. All of the polymers had excellent solubility in common organic solvents. The UV and PL spectra for P-Ct were 312 and 400 nm while for P-OC*n* they were around 328 and 420 nm in the film. There was no red shift in the PL spectrum of P-Ct after heat treatment which maybe related to the jacketed structure. All of the polymers showed high PL quantum yields in THF solution. From the cyclic voltammetry measurement at room temperature, HOMO levels of the polymers were varied from −5.66 to −6.12 eV, LUMO levels were varied from −2.45 to −2.81 eV. Furthermore, the influence of the alkoxyl lengths in four different device configurations was compared. For the device configuration **c**: ITO/PVK/P-OC8/Ca/Ag, the maximum luminance and maximum external quantum efficiency were obtained for P-OC8 which maybe related to the easier electron injection and transport. Efficiency of P-OC8 was not improved with device **d** which proved the electron transporting characteristics of P-OC8.

Keywords: Mesogen-jacketed polymers (MJP); 1,3,4-Oxadiazole; Polymer light-emitting diodes (PLEDs)

1. Introduction

Polymer light-emitting diodes (PLEDs) have made rapid progress since the first report of polymer light-emitting diodes (LEDs) based on poly(*p*-phenylenevinylene) PPV by Burroughes et al. [1]. Polymer materials have been expected to be suitable for LEDs because of their good processability and the ease of fabrication based on solution processing techniques and the application in flexible flat panel displays [2,3]. PLED materials are generally categorized into conjugated main chain polymers and side chain polymers. Conjugated polymers such as poly(1,4-phenylenevinylene) (PPV), polyalkyl fluorine (PAF) and poly(*p*-phenylene) (PPP) have been most widely used as the emissive layer for the light-emitting diodes because of low turn-on voltage, high brightness, high luminescence efficiency [4d], mechanical strength and amorphous properties [4,5]. However, conjugated polymers still have problems in that their conjugated backbones tend to make the polymer rigid and hence poor solubility which makes them difficult to process into good thin films [6]. Compared to conjugated polymers, non-conjugated side chain polymers which have an emitting moiety linked via a short spacer or without it to non-conjugated backbone (major polyvinyl backbone) can be synthesized via free-radical chain polymerization. They have the

* Corresponding authors.
E-mail addresses: fanxh@pku.edu.cn (X. Fan), dczou@pku.edu.cn (D. Zou), qfzhou@pku.edu.cn (Q. Zhou).

0032-3861/$ - see front matter © 2007 Elsevier Ltd. All rights reserved.
doi:10.1016/j.polymer.2007.07.071

following advantages [7c]: the synthetic route would be simpler than that used for main chain polymers, the solubility would be dominated by the nature of the backbone, the emission wavelength would be predetermined, and crystallization of the chromophore with concomitant degradation of the diode (in comparison with small molecular weight sublimable systems) would be prevented. In addition, a variety of possible pendant molecules, an electroluminescent group could be placed on every repeat unit or in a controlled frequency along the backbone, and the photoconductivity of the pendant-electron systems [7–10]. However, because of the flexible backbone of side chain polymers, chains tend to aggregate and less conjugation of side chains leads to high turn-on voltage and low brightness and efficiency [11]. To the present, side chain polymers are mainly investigated as just hole transporting materials or electron transporting materials [12].

Mesogen-jacketed polymer is a kind of polymer in which [13] mesogenic units are attached laterally to the gravity centers of the main chain without or with only short spacers; the main chain of mesogen-jacketed polymers is forced to extend and to take rigid conformation because of high population of both bulky and rigid side groups around the backbone. Therefore, we suppose that this special structure can make up for the disadvantages of poor solubility and synthesis problems of main chain conjugated polymers. In addition, the jacketed structure and extended main chain can make the side groups confined and ordered, which suppress intermolecular interaction and maintain the conjugation. On the other hand, the polymers can be processed very easily, for example, by spin coating or printing.

From the molecular design aspect, a problem of LED is that electron injection and transport are much more difficult than hole injection and transport. In order to increase the electron injection and transport abilities, over the past few years, many efforts have been attempted to develop novel materials with improved balance between charge injection and transport in LED devices. In 1989, it was reported that 2-(biphenyl-4-yl)-5-(4-*tert*-butylphenyl)-1,3,4-oxadiazole (PBD) possesses high photoluminescence quantum yields, good thermal stability and chemical stabilities [14]. Since this report, 1,3,4-oxadiazole (OXD) moieties have been employed as an electron transporting unit in the study of PLEDs [4d,15]. Schulz et al. [15g] introduced 1,3,4-OXD units to the main chain conjugated polymers and achieved high electron affinities E_A's −2.8–3.6 eV and high ionization potential I_P −6.0 eV. However, these cannot be used as electron transporting materials because of poor solubility. And later, Strukelj et al. [15c] introduced 1,3,4-OXD units into the side chain of PMMA backbone, which improved T_g and when used as electron transporting materials, enhanced the lifetime of devices.

In this paper, we report the optical, electrochemical and electroluminescent properties of a series of novel mesogen-jacketed polymers P-Ct and P-OC*n* containing 1,3,4-OXD. Furthermore, we compared the influence of their alkoxyl lengths in four different device configurations.

2. Experimental section

2.1. Materials

All the polymers (denoted as P-Ct and P-OC*n* in Fig. 1) were obtained by conventional solution radical polymerization. All of the monomers were qualified by IR, ^{1}H NMR and elemental analysis, for example, M-Ct, IR (cm^{-1}): 3075, 3043 ($\nu_{Ar\text{-}H}$, $\nu_{C=CH}$); 2955, 2873 ($\nu_{-CH_2,\ -CH_3}$); 1609, 1560, 1498, 1476 (phenyl $\nu_{C=C}$); 1347 ($\nu_{C=N}$); 1303, 1257, 1175 (ν_{C-O-C}). ^{1}H NMR (δ, ppm): 1.39 (s, 18H, $-CH_3$), 5.62, 5.99 (d, 2H, $=CH_2$), 7.93 (m, 1H, $-CH=$), 8.16, 8.08, 7.04 (m, 10H, Ar-H), 8.43 (s, 1H, Ar-H). Elemental analysis, found (calcd.): C%: 76.02 (76.16), H%: 6.53 (6.39), N%: 10.99 (11.10) [18].

To improve purity and device performance, the resulting polymers were further purified by multiple precipitations with different solvents including methanol, alcohol, and hexane to remove low molecular weight polymers and impurities. By carrying out these processes, highly purified and narrowly polydisperse polymers were obtained. Table 1 summarizes the polymerization results and thermal properties of P-Ct and P-OC*n*. The molecular-average molecular weights (M_n) and polydispersities (PDIs) of the resulting polymers after molecular fractionation were found to be $(7.2–19.6) \times 10^{-4}$ and 1.2–1.5, respectively. The polymers showed decomposition temperatures (T_d, 5% weight loss) from 381 to 394 °C and T_g from 161 to 222 °C. The synthesis and phase transitions, and phase structures of the polymers will be published in a separate paper.

2.2. Measurement and characterization

Absorption spectra were measured using a CARY 1E spectrophotometer of Australian Varian Company, with the wavelength between 190 and 900 nm and the width of the spectral band between 0.2 and 4.0 nm.

Photoluminescence (PL) spectra were obtained using a Hitachi F-4500 luminescence spectrometer. Fluorescence quantum yield of the polymer was determined by using 9,10-diphenylanthracene (dissolved in *n*-hexane with a concentration of 10^{-6} M, assuming ϕ_{PL} of 1.00 ± 0.05) as a standard compound. The fluorescence quantum yields were calculated according to the following formula:

$$\phi = \phi_r \left(\frac{A}{A_r}\right)\left(\frac{OD_r}{OD}\right)\left(\frac{n^2}{n_r^2}\right)$$

where ϕ is the fluorescence quantum yield, A is the fluorescence integral area, OD is the absorbance, and n is the

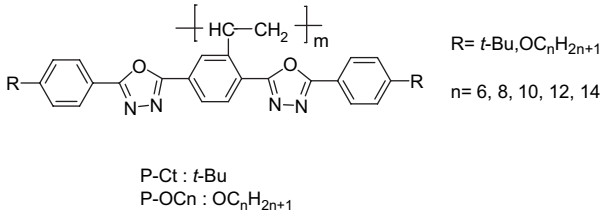

Fig. 1. Chemical structure of P-Ct and P-OC*n* used in this study.

Table 1
Molecular weight, PDI and thermal properties of polymers

Samples	$M_n \times 10^{-4}$ [a]	PDI[a]	T_g [b] (°C)	T_d [c] (°C)
P-Ct	14.3	1.4	222	394
P-OC6	18.6	1.3	184	392
P-OC8	12.2	1.4	180	389
P-OC10	23.5	1.2	171	388
P-OC12	12.1	1.3	167	387
P-OC14	10.8	1.5	161	381

[a] M_n and PDI of the polymers were determined by GPC using polystyrene standards.
[b] Evaluated by DSC during second heating cycle at a rate of 10 °C/min.
[c] The temperature at which 5% weight loss of the sample was reached from TGA under nitrogen atmosphere.

refractive index. The subscript r refers to the reference substance whose fluorescence quantum yield is already known.

Cyclic voltammetry (CV) was performed on a computer-controlled EG&G potential/galvanostat model 283 electrochemical analyzer in a solution of tetrabutylammonium perchlorate (0.1 M) in acetonitrile at a scanning rate of 50 mV/s. The polymer film as a working electrode was coated on a square platinum electrode by casting and then dried in air. Platinum wire was used as a counter electrode, and Ag/AgCl (AgCl was plated on silver wire) was used as a reference electrode. Prior to each series of measurements, the cell was deoxygenated with argon. Ferrocene/ferrocenium (Fc/Fc^+) is known to be 4.8 eV below the vacuum level [19] and was used as a calibration reference. After CV measurements of polymers, two drops of ferrocene in acetonitrile (5 mM) were added and measured for calibration. The half-wave potential of Fc/Fc^+ was measured to be 0.4 eV.

2.3. Device fabrication and characterization

The fabrication process of the diodes followed a standard procedure which is given below. The patterned ITO (indium tin oxide) substrate was cleaned with detergents and deionized water, and finally treated with UV–ozone for about 25 min. PEDOT (purchased from Aldrich) was spin coated on the precleaned ITO substrate and dried by baking in air at 120 °C for 10 h. Then, the polymer was spin cast from toluene solution (10 mg/ml) through a 0.45 μm Teflon filter. The thickness of the spin-coated film was controlled by regulating the spinning speed. Then the coated ITO was transferred into a deposition chamber with a base pressure of 1.0×10^{-6} Torr, Mg:Ag layer was evaporated onto the polymer layer. The emitting area was 2 mm × 2 mm. The EL spectra were measured with a spectrofluorometer FP-6200 (JASCO). A source-measure unit R6145 (Advantest), multimeter 2000 (Keithley) and luminance meter LS-110 (Minolta) were used for *I–V–L* measurements. Relative luminance was directly detected by using a multifunctional optical meter 1835-C (Newport).

The device configurations used in this study are

a: ITO/PEDOT/polymer/Mg:Ag (10:1, 150 nm)/Ag (10 nm),
b: ITO/PEDOT/polymer/Ca (20 nm)/Ag (80 nm),
c: ITO/PVK/polymer/Ca (20 nm)/Ag (80 nm),
d: ITO/PEDOT/P-OC8/TPBI (15 nm)/AlQ (20 nm)/Mg:Ag (10:1, 150 nm)/Ag (10 nm).

3. Results and discussion

3.1. Optical properties of the polymers

The optical absorption spectra of the polymers in solution and in films are shown in Fig. 2. Maximum absorption wavelength λ_{max} was 312 nm for P-Ct and 328 nm for P-OC*n* in films and 309 nm for P-Ct and 320 nm for others in THF solution. The red shift of the absorption spectra in thin film can be attributed to the π-conjugated OXD segment. The alkoxyl end length exerts little influence on the ground-state electronic transitions, the absorption spectra of P-OC8 and P-OC10 are very similar to that of P-OC12 and P-OC14. Because of the stronger electron-donating capabilities of the alkoxyl end groups than *tert*-butyl end groups, there was a red shift both in solution and in films for P-OC*n* than P-Ct.

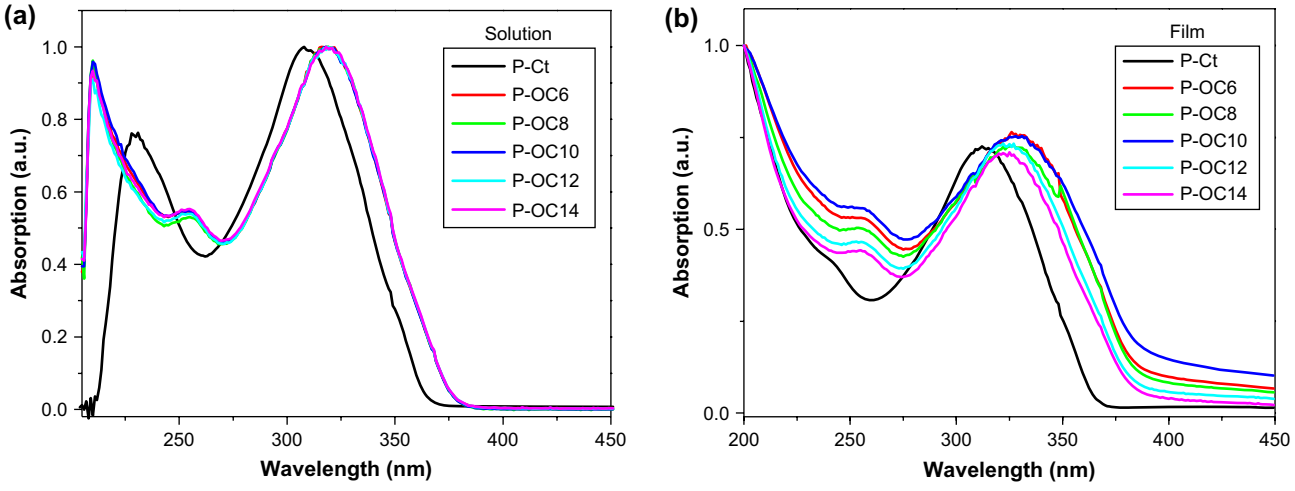

Fig. 2. UV–vis absorption spectra of the polymers: (a) in THF solution (1 mg/100 ml) and (b) in film state.

In order to further investigate the effect of the alkoxyl end groups on the optical properties, PL spectra of the polymers in solution and in films are shown in Fig. 3. The PL spectra of the polymers in films were only slightly red shifted with respect to their corresponding spectra in solution, indicating that there were no noticeable molecular conformation changes from solution to the solid state. Similar to absorption spectra, all of the polymers showed maximum emission at around 410 and 420 nm in solution and in films except for P-Ct at around 390 and 400 nm, respectively. In order to investigate the thermal stability, we treated the film of P-Ct from 30 to 190 °C at 2 °C/min and then held at 190 °C for 0.5 h, and then cooled from 190 to 30 °C at the same rate. The PL spectra of the treated film and untreated film are presented in Fig. 3c. As shown, there was no red shift after heat treatment and the peak became narrower. This indicated that the jacketed structure of P-Ct suppressed the aggregate formation under heat treatment.

3.2. Electrochemical properties

To investigate the charge injection and transport of P-Ct and P-OC*n*, it is very important to determine the energy band diagrams of the HOMO and LUMO binding energy levels by using cyclic voltammetry (CV) electrochemical measurements. CV can be used to estimate relative ionization potentials I_P's and electron affinities E_A's of the conjugated chromophore in the side chain. To a first approximation, the oxidation potential of a material (as measured by CV) can be related to the I_P and the highest occupied molecular orbital (HOMO) energy level. A similar relationship maybe made with the reduction potential, as well as with the E_A and the lowest unoccupied molecular orbital (LUMO) energies. However, the presence of solvent and counterions, as well as the kinetic nature of electrode processes in CV, makes the correlation only approximate. One check on the reliability of this relationship is that the difference between the oxidation potential and the reduction potential should be equal to the optical band gap. The cyclic voltammograms of polymers are illustrated in Fig. 4. The energy levels of P-Ct and P-OC*n* are summarized in Table 2.

Unfortunately, the oxidation processes were hardly recorded after many attempts. The LUMO levels of the polymers were calculated according to the empirical formula (energy level value of Fc under vacuum is 4.8 eV, the half-wave potential of Fc/Fc^+ was 0.4 eV):

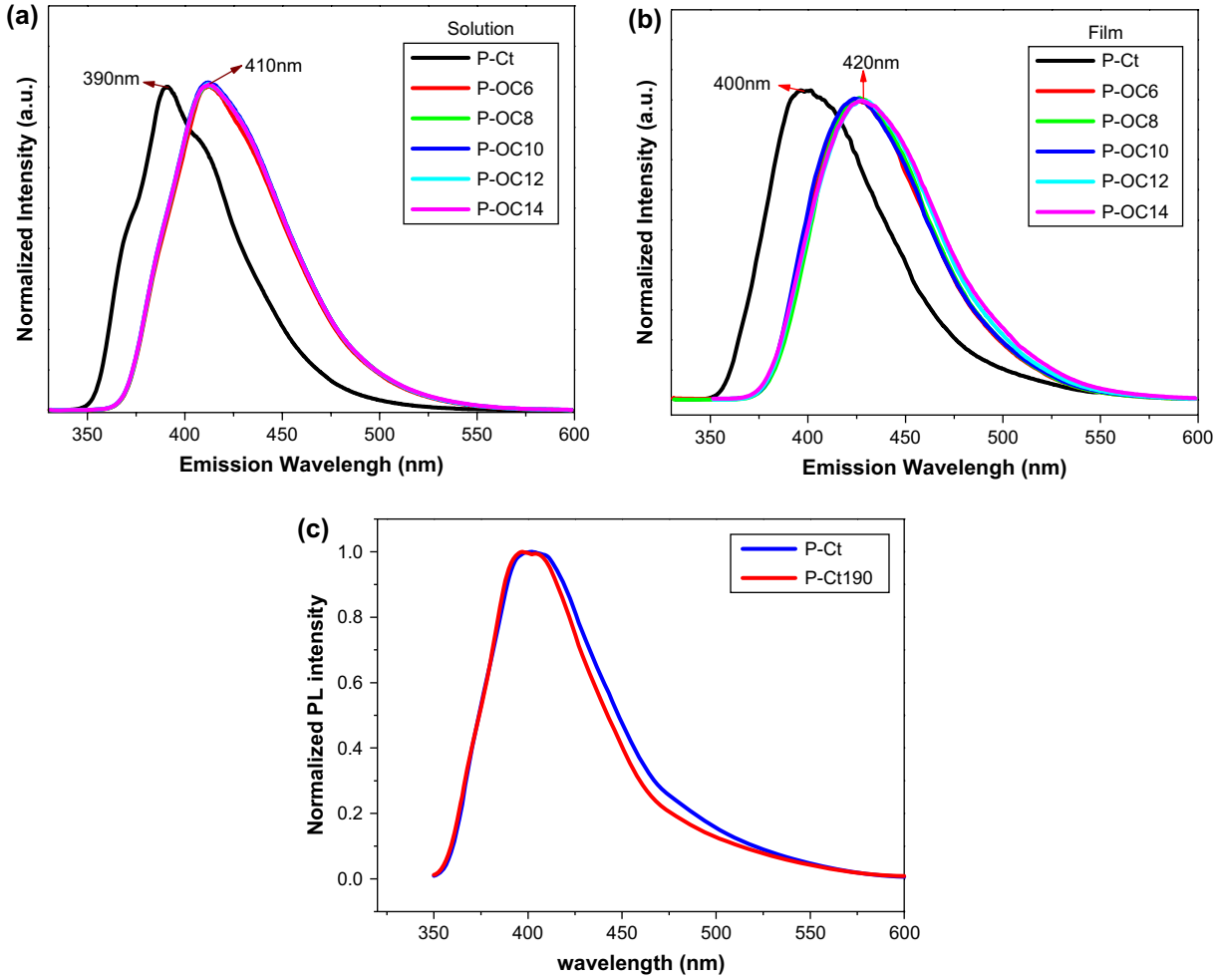

Fig. 3. PL spectra of polymers: (a) in solution, (b) in film state and (c) the treated film and untreated film for P-Ct. (Solution: $\lambda_{ex} = 310$ nm for P-Ct and 320 nm for P-OC6–P-OC14. Film: $\lambda_{ex} = 310$ nm for P-Ct and 330 nm for P-OC6–P-OC14.)

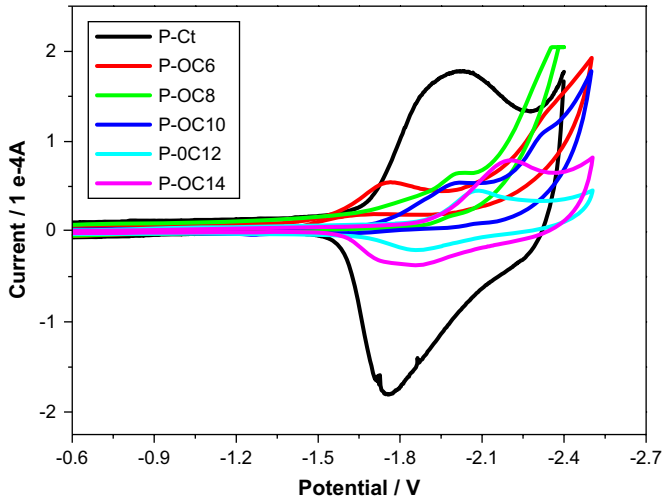

Fig. 4. Cyclic voltammograms of polymers.

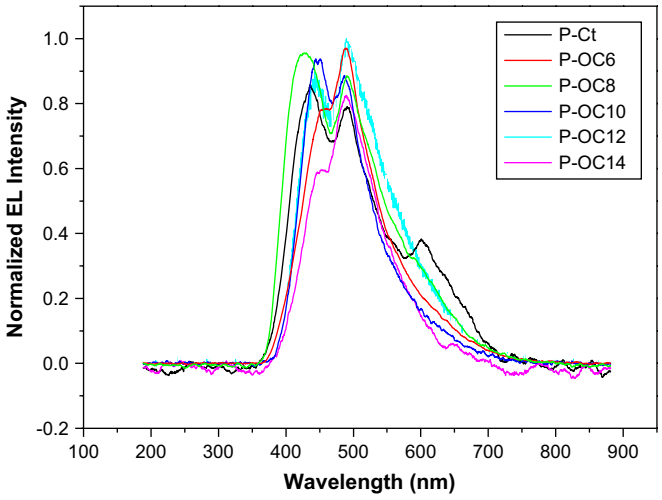

Fig. 5. EL spectra of P-Ct and P-OC*n*.

$$E_{\mathrm{HOMO}} = I_{\mathrm{P}} = -\left[E^{\mathrm{ox}}_{\mathrm{onset}} + (4.8 - 0.4)\right]\ \mathrm{eV}$$

$$E_{\mathrm{LUMO}} = E_{\mathrm{A}} = -\left[E^{\mathrm{red}}_{\mathrm{onset}} + (4.8 - 0.4)\right]\ \mathrm{eV}$$

Band gaps were estimated from the UV–vis absorption edges for the film-state polymers. They showed that the longer the alkyl side chain in polymers, the higher the HOMO and LUMO levels from P-OC6 to P-OC14. However, the polymer P-OC8 showed a deviation from this tendency, which maybe due to the different phase structures, P-Ct formed hexatic columnar nematic (Φ_{HN}) phase, P-OC8 formed smectic A (S_{A}) phase, P-OC6 formed complex phases [18]. Different phase structures led to different π^* orbitals of P-OC*n*.

3.3. Light-emitting diodes with the polymers

To investigate the EL properties of P-Ct and P-OC*n*, from the HOMO levels of the polymers, we investigated three device configurations **a**, **b** and **c**. Fig. 5 shows the normalized EL spectra of P-Ct and P-OC*n* in device configuration **c**: ITO/PVK/polymer/Ca/Ag. EL spectra of all the polymers were similar. The same EL maximum peaks at around 440 and 490 nm are owing to the same effective conjugation length of the mesogenic units. P-Ct showed an additional peak at around 601 nm which maybe due to the interaction between P-Ct and electrode [17], for heat treatment was impossible. EL spectra of all the polymers showed a 20 nm red shift than their PL spectra. This change in EL spectrum was due to the injected current density, which results in an extended effective conjugation length [4d]. All of the polymers showed an additional peak at around 490 nm which is attributed to charge recombination and emission occurs on the chromophore of P-OC*n* [16a].

Fig. 6 shows the luminance–voltage characteristics of P-OC14 and the current efficiency–current density characteristics of P-OC8 in various device configurations (**a**, **b**, **c** and **d**). For P-OC14, the maximum luminescence of device **c** is 20 times higher than device **a**; and for P-OC8, the maximum current efficiency (cd/A) of device **c** is 10 times higher than device **a**. The maximum EL efficiencies of all the polymers with device **c** are 10 times or much higher than device **a**. The results are attributed to smaller barrier for hole injection from PVK into polymer (0.16–0.5 eV) than from PEDOT into polymer (0.66–1.1 eV). On the other hand, the barrier for electron injection from Ca into polymer (0.19–0.55 eV) is smaller than that from Mg into polymer (0.89–1.25 eV). Therefore, we achieved the best EL performance when we used PVK as the HTL (hole transporting layer) and Ca as the anode. In addition, we designed device configuration **d**, in which an electron transporting layer was added for electron injection and transport. However, the EL efficiency of device **d** is lower than devices **b** and **c**. It can be explained from the electron transporting characteristics of OXD units. The electron transporting characteristics are still under investigation.

The luminance–voltage and current efficiency–current density curves of P-Ct and P-OC*n* based on device **c** are shown in Fig. 7. From device **c**, the maximum brightness and the best efficiency for P-OC8 were achieved, for P-OC8 has energy

Table 2
Electrochemical and optical properties of P-Ct and P-OC*n*

Samples	UV λ (nm) max peak	UV λ (nm) onset	Band gap (eV)	E_{red} (V vs. Ag/AgCl)	LUMO (eV)	HOMO (eV)
P-Ct	312	365	3.40	−1.67	−2.73	−6.12
P-OC6	328	387	3.20	−1.74	−2.66	−5.86
P-OC8	327	385	3.22	−1.59	−2.81	−6.03
P-OC10	328	386	3.21	−1.75	−2.65	−5.86
P-OC12	327	384	3.23	−1.83	−2.57	−5.80
P-OC14	327	383	3.24	−1.92	−2.48	−5.72

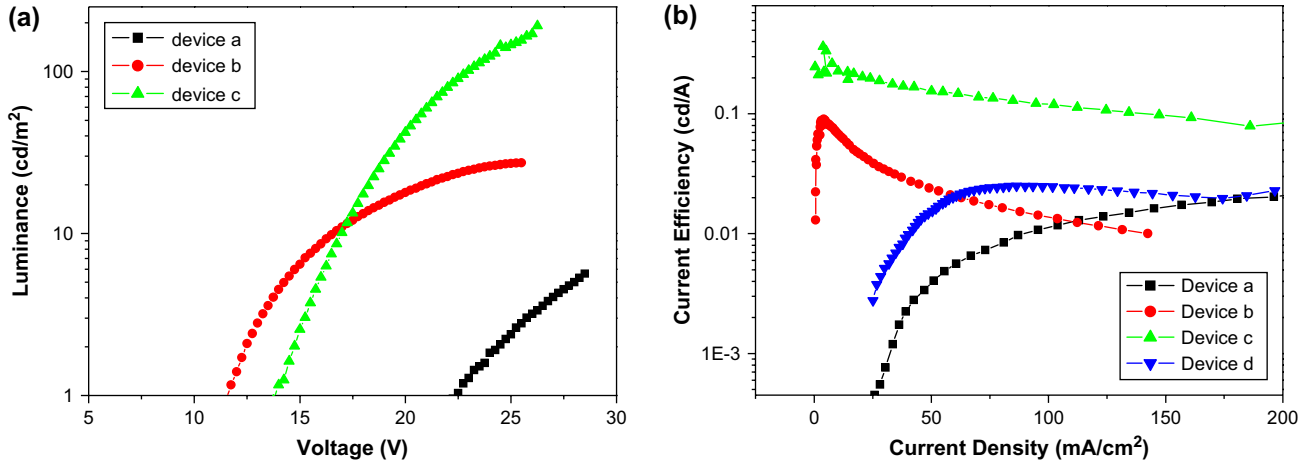

Fig. 6. (a) Luminance–voltage curves of P-OC14 in device configurations **a**, **b**, **c** and (b) current efficiency–current density curves of P-OC8 in device configurations **a**, **b**, **c** and **d**.

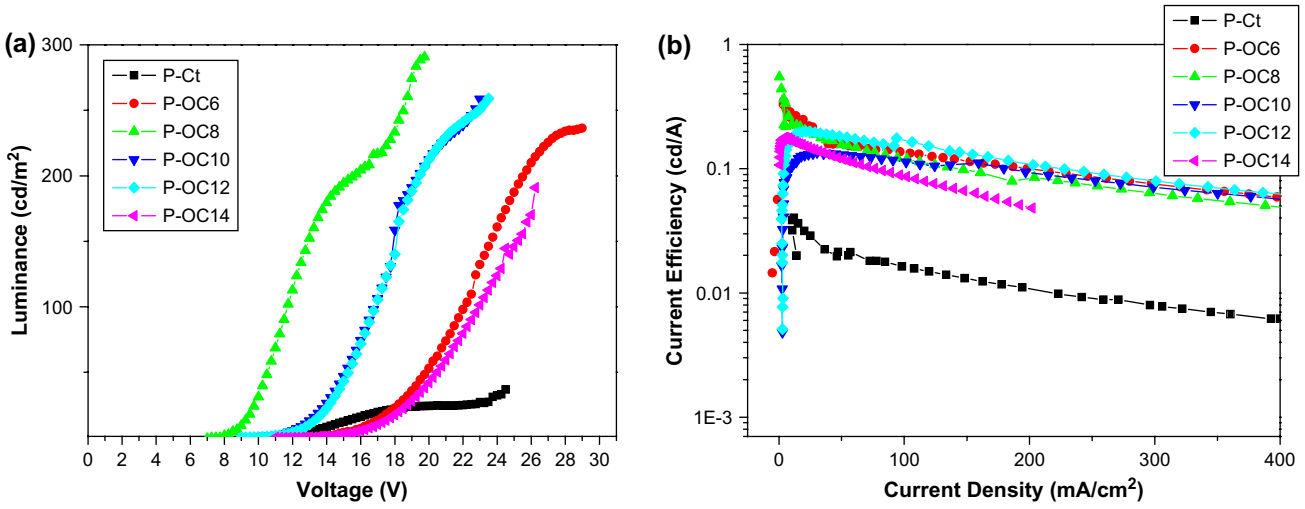

Fig. 7. (a) Luminance–voltage and (b) current efficiency–current density curves of P-Ct and P-OC*n* in device **c**.

barriers of only 0.09 eV for an electron injection. P-OC6 has energy barriers of 0.34 eV for an electron and 0.36 eV for a hole, and the energy barriers of P-OC6 are more balanced than P-OC12 and P-OC14. Moreover, it maybe related to the solubility and intermolecular interaction. As the length of the alkoxyl end groups increased, the solubilities increased and intermolecular interaction increased.

Table 3 shows the EL characteristics of all the polymers based on device **c**. P-Ct which had the highest symmetry and rigid structure exhibited the poorest performance. Other polymers exhibited high brightness and high efficiency. It is showed that onset voltages are increased by increasing the length of alkyl chain unit attached on OXD moieties except for the case of P-Ct. The better electron transporting property of P-Ct with shorter alkyl chain may attribute to the low onset voltage. However, even though P-OC6 has the shortest alkyl chain, the polymer shows rather high onset voltage of 13.6 V. The relatively larger molecular weight and polydispersity of P-OC6 affected its electron transporting property which maybe the reason for the high onset voltage. Shirota et al. [7a,16a] reported single layer LED characteristics of side chain polymers PM6-OXD-MA and PM6-OXD-PA containing

Table 3
Electroluminescent characteristics of P-Ct and P-OC*n*

Samples	U_{onset} (V)	L_{max} (cd/m^2)	$\eta_{L_{max}}$ (lm W^{-1})	$\eta_{I_{max}}$ (cd/A)	CIE coordinate	η_{extmax} (%)	λ (nm) (low voltage)
P-Ct	11.2	36.8	1.0×10^{-2}	4.0×10^{-2}	0.175, 0.147	1.0×10^{-1}	440, 494
P-OC6	13.6	236.3	6.5×10^{-2}	3.5×10^{-1}	0.169, 0.208	2.3×10^{-1}	451, 492
P-OC8	7.9	290.8	7.6×10^{-2}	3.6×10^{-1}	0.225, 0.244	2.4×10^{-1}	433, 490
P-OC10	10.5	258.7	2.9×10^{-2}	1.4×10^{-1}	0.189, 0.204	8.9×10^{-2}	437, 490
P-OC12	10.7	259.0	4.2×10^{-2}	2.0×10^{-1}	0.190, 0.207	9.5×10^{-2}	440, 490
P-OC14	13.8	190.9	4.5×10^{-2}	2.7×10^{-1}	0.190, 0.273	1.1×10^{-1}	450, 492

both electron and hole transport units. They achieved maximum brightness of 13 cd/m^2 and external quantum efficiency of 3.0×10^{-4}% and maximum brightness of 30 cd/m^2 separately. Rubner et al. [16b] investigated double layer EL characteristics of side chain polymer polynorbornene, they achieved maximum luminance of 675 nW and maximum external quantum efficiency of 5.0×10^{-4}%. However, P-OC8 achieved maximum brightness of 290.8 cd/m^2 and external quantum efficiency of 0.24%. Mesogen-jacketed polymers P-OC*n* have some rigid properties in the main chain which would be easy for carrier transport and the bulk rigid side groups could reduce intermolecular interaction. The results indicate that P-OC*n* polymers are promising materials for PLED applications.

4. Conclusions

We have investigated the optical and electroluminescent properties of a series of mesogen-jacketed polymers P-Ct and P-OC*n*. The UV–vis absorption and PL results reveal that they are good blue light-emitting materials and show high thermal stability and fluorescence quantum yields (over 60%). Electrochemical measurements show that all of the polymers have low LUMO energy levels and good electron transporting characteristics. According to the HOMO and LUMO levels, we designed four device configurations. Among them, device configuration **c** shows the best performance of all the polymers and maximum external quantum efficiency was 0.24% for P-OC8. These results are good compared to side chain polymers reported. The introduction of PVK layer improved hole injection and transport which enhanced the recombination and radiation. In order to design a high-performance PLED, further modification and optimization of the EL devices with P-OC*n* are in progress.

Acknowledgment

This work was supported by the National Natural Science Foundation of China (Grant Nos.: 20574002, 20634010) and the Science Research Fund of the Chinese Ministry of Education (Grant No.: 104005) and by NSF, 863, 973 programs of PR China (Nos. 50125310, 90401028, 2002AA324080 and 2002CB613405).

References

[1] Burroughes JH, Bradley DDC, Brown AR, Marks RN, Mackay K, Friend RH, et al. Nature 1990;347:539.
[2] (a) Braun D, Heeger AJ. Appl Phys Lett 1991;58:1982;
(b) Suzuki T. J Appl Phys 2006;99:111101.
[3] For reviews, see:
(a) Friend RH, Gymer RW, Holmes AB, Burroughes JH, Marks RN, Taliani C, et al. Nature 1999;397:121;
(b) Shirota Y. J Mater Chem 2000;10:1;
(c) Mitschke U, Bäuerle P. J Mater Chem 2000;10:1471.
[4] (a) Kim JH, Park JH, Lee H. Chem Mater 2003;15:3414;
(b) Mikroyannidis JA, Spiliopoulos IK, Kasimis TS, Kulkarni AP, Jenekhe SA. Macromolecules 2003;36:9295;
(c) Lee YZ, Chen X, Chen SA, Wei PK, Fann WS. J Am Chem Soc 2001;123:2296;
(d) Jin SH, Kim MY, Kim JY, Lee K, Gal YS. J Am Chem Soc 2004;126:2474.
[5] (a) Ding J, Day M, Robertson G, Roovers J. Macromolecules 2002;35:3474;
(b) Setayesh S, Grimsdale AC, Weil T, Enkelmann V, Müllen K, Meghdadi F, et al. J Am Chem Soc 2001;123:946;
(c) Peng Z, Galvin ME. Acta Polym 1998;49:244;
(d) Xia C, Advincula R. Macromolecules 2001;34:6922;
(e) List EJW, Holzer I, Tasch S, Leising G, Scherf U, Müllen K, et al. Solid State Commun 1999;109:455;
(f) Kido J, Kohda M, Nagai K. Appl Phys Lett 1992;61:761.
[6] Bisberg J, Cumming WJ, Gaudiana RK, Hutchinson KD, Ingwall RT, Kolb ES, et al. Macromolecules 1995;28:386.
[7] (a) Kawamoto M, Mochizuki H, Shishido A, Tsutsumi O, Ikeda T, Lee B, et al. J Phys Chem B 2003;107:4887;
(b) Ling QD, Cai QJ, Kang ET, Huang W. J Mater Chem 2004;14:2741;
(c) Akcelrud L. Prog Polym Sci 2003;28:875.
[8] (a) Oh SY, Lee CH, Kim HM, Choi JW, Rhee HW. Mol Cryst Liq Cryst 2000;349:483;
(b) Oh SY, Lee CH, Kim HM, Choi JW, Rhee HW. Synth Met 2001;117:95.
[9] Oh SY, Kim HM, Lee CH, Choi JW, Rhee HW, Kim HS. Polymer 2000;24:90.
[10] Yamaguchi M, Nagatomo T. Thin Solid Films 2000;363:21.
[11] (a) Lee JK, Hwang DH, Hwang J, Jung HK, Zyung T, Park SY. Synth Met 2000;111–112:489;
(b) Bouche CM, Schott M. Synth Met 1996;81:191.
[12] (a) Bellmann E, Shaheen SE, Grubbs RH, Marder SR, Kippelen B, Peyghambarian N. Chem Mater 1999;11:399;
(b) Greczmiel M, Strohriegl P, Meier M, Brutting W. Macromolecules 1997;30:6042;
(c) Shaheen SE, Jabbour GE, Anderson JD, Bellmann E, Grubbs RH. Appl Phys Lett 1999;74:3212.
[13] Zhou QF, Li HM, Feng XD. Macromolecules 1987;20:233.
[14] Adachi C, Tsutsui T, Saito S. Appl Phys Lett 1989;55:1489.
[15] (a) Pei Q, Yang Y. Adv Mater 1995;7:559;
(b) Buchwald E, Meier M, Karg S, Pösch P, Schmidt HW, Strohriegl P, et al. Adv Mater 1995;7:839;
(c) Strukelj M, Papadimitrakopoulos F, Miller TM, Rothberg LJ. Science 1995;267:1969;
(d) Kim ST, Hwang D, Li XC, Gruner J, Friend RH, Holmes AB, et al. Adv Mater 1996;8:979;
(e) Cao Y, Parker ID, Yu G, Zhang C, Heeger AJ. Nature 1999;397:414;
(f) Tzanetos NP, Kallitsis JK. J Polym Sci Part A Polym Chem 2005;43:1049;
(g) Schulz B, Bruma M, Brehmer L. Adv Mater 1997;9:601.
[16] (a) Mochizuki H, Hasui T, Kawamoto M, Ikeda T, Adachi C, Taniguchi Y, et al. Macromolecules 2003;36:3457;
(b) Boyd TJ, Geerts Y, Lee JK, Fogg DE, Lavoie GG, Schrock RR, et al. Macromolecules 1997;30:3553.
[17] Kwon KY, Lin X, Pawin G, Bartels L. Langmuir 2006;22:857.
[18] Chai CP, Wang J, Fan XH, Chen XF, Zhou QF. Acta Polym Sin 2006;3:532.
[19] Sun QJ, Wang HQ, Yang CH, Li YF. J Mater Chem 2003;13:800.